Supporting Information

Fullerene-free organic solar cells with an efficiency of 3.7% based on a low-cost geometrically planar perylene diimide monomer

R. Singh[a], E.Aulicio-Sarduy[a], Z. Kan[a], T. Ye[a], R.C. I. MacKenzie[b], P. E. Keivanidis[a] *

Materials and Methods

Materials: The PBDTTT polymers (both PBDTTT-E-O and PBDTTT-CT) and the PDI were purchased from Solarmer Energy, Inc. The 1,8-diiodooctane additive, the poly(styrene) matrix and the metal oxides of ZnO and V_2O_5 were purchased from Sigma Aldrich. All purchased materials were used as received without further purification steps.

Solution-processed photoactive layer preparation: The photoactive layers of the PBDTTT:PDI blend films were prepared by co-dissolving the polymer and the PDI components in chloroform at 40 °C with a solution concentration of 20 mg/ml and with a weight polymer:PDI ratio of 3:7. The polymer:PDI solution was then filtered with a 0.2 μm pore diameter PTFE filter and deposited either on quartz or on glass/ITO/PEDOTT:PSS substrates by spin-coating and they were annealed at 100 °C for 15 min. The effect of additive was studied by varying the DIO content in the PBDTTT-CT:PDI solution, between 0 vol% and 1.2 vol%. The film thickness of the polymer:PDI films was kept between 90 nm – 100 nm as determined by a Dektak 150 profilometer. A similar procedure was followed for fabricating PS:PDI control films of the same weight ratio and of comparable film thickness. UV-Vis and time-integrated PL spectroscopic characterization of the prepared films was performed like previously described. [1]

Solar cell fabrication and characterization: Inverted device geometries of the type glass/ITO/ZnO/PBDTTT:PDI/V_2O_5/Ag with annealed photoactive layers, were prepared and

characterized by means of external quantum efficiency, photovoltaic response under simulated solar illumination and photoexcitation dependent time-integrated short-circuit photocurrent, like previously described. [1] The electron-selective ZnO layer [2] was spin-coated from solution on the plasma etched glass/ITO substrates. Following the deposition of the PBDTTT:PDI photoactive layers, subsequent depositions of 2 nm thick V_2O_5 [3] and 70 nm thick Ag layers were performed in vacuum (2×10^{-6} mbar) by thermal evaporation. For all devices, the active area of the pixels as defined by the overlap of anode and cathode area was 5.25 mm^2. Annealing of the devices were performed in a nitrogen-filled glovebox by placing them on a hotplate in at 100^{o}C for 15 min. All devices were encapsulated before moving out of glovebox. The electrical characterization of the fabricated solar cells was performed by means of external quantum efficiency (EQE) and by determining the basic photovoltaic parameters under simulated solar illumination by using an Oriel Sol3A Class AAA solar simulator (AM1.5G, 0.98 Suns). Mobility measurements were performed based on single carrier devices with photoactive layers prepared in an identical fashion to the OPV devices. The charge carrier mobility for each device was determined based on the space charge limited current method. [1] Electron-only devices were prepared with electrodes of glass/ITO/ZnO and Ca/Al whereas hole-only devices were prepared with electrodes of glass/ITO/PEDOT:PSS and Au.

Light intensity dependent J-V characterization: A diode pumped solid state laser (DPGL2010F, Lambda Photometrics, 10 mW, 1 mm diameter spot size)) was used for photoexciting the devices at 532 nm and the photocurrent J-V curves were recorded with a Keithley electrometer. The monochromatic light intensity was attenuated with the use of neutral density filters of known transmittance values. For each device pixel several measurements were repeated for ensuring the stable response of the device photocurrent. All measurements were performed in ambient and a good reproducibility of the measured

photocurrent was found for the OPV devices that were properly encapsulated with epoxy and glass.

Transient short-circuit photocurrent characterization: Transient short-circuit photocurrent measurements were performed after photoexciting the OPV devices with the output of an optical parametric oscillator (Spectra-Physics VersaScan Midband 120) pumped by the third harmonic of a Nd:YAG Laser (Spectra-Physics INDI-40-10-HG), at 532 nm by a train of 10 ns pulses at a repetition rate of 10 Hz, with average pulse energy of 700 nJ/pulse. During photoexcitation, the OPV device was directly connected to a two-channel digital oscilloscope (Agilent 3000) with an input impedance of 50 Ω and the laser signal was monitored with a reference photodiode. Both signals of the OPV device photocurrent response and the reference photodiode were recorded by the oscilloscope.

Transient open-circuit voltage characterization: transient open-circuit voltage measurements under white light background illumination were performed after photoexciting the OPV devices with the output of an optical parametric oscillator pumped by the third harmonic of a Nd:YAG Laser, at 532 nm by a train of 10 ns pulses at a repetition rate of 10 Hz, with average pulse energy of 14 μJ/pulse. During photoexcitation, the OPV device was directly connected to a two-channel digital oscilloscope with an input impedance of 1 MΩ. A Xenon lamp was used as the source of the background illumination light and a Solar reference cell (SRC-1000-TC-QZ-N), was used for determining the intensity of the white light sent to the OPV device. During the measurements the intensity of the white light was selectively attenuated with the use of neutral density filters of known transmittance.

Atomic force microscopy characterization: Atomic Force Microscopy Imaging (AFM): Surface topography of all blend films was studied by atomic force microscopy (AFM) using an Agilent 5500 in tapping mode under ambient conditions. Topography and phase images were recorded simultaneously.

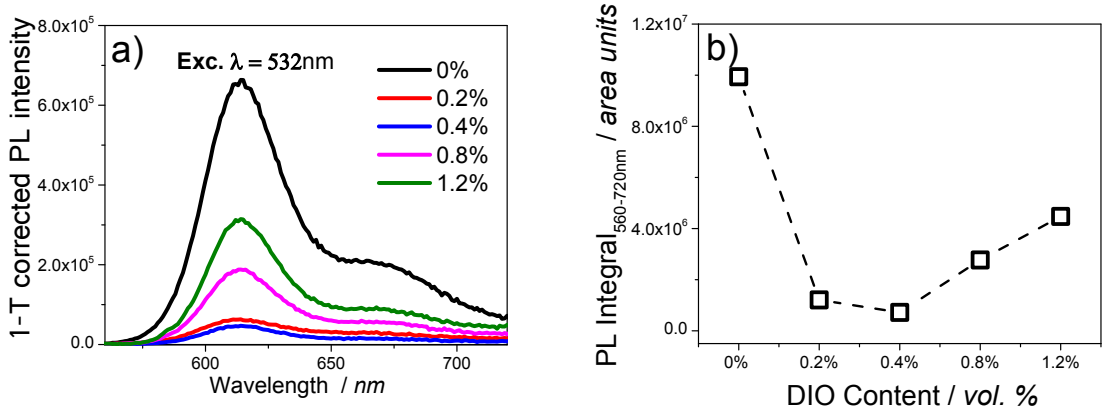

Figure S.1 a) 1-T corrected photoluminescence (PL) spectra, b) integrated PL spectrum (λ_{range} = 560 - 720nm) of the PBDTTT-CT: PDI (3:7) blend system annealed at 100 °C, with different vol. % of DIO additive. The concentration of DIO additive varied from 0 vol. % to 1.2 vol. %.

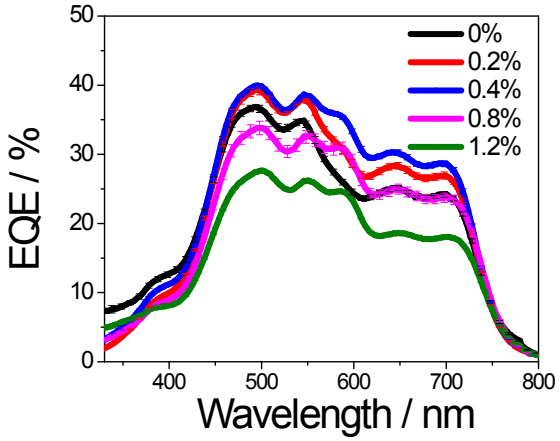

Figure S.2 External quantum efficiency spectra of organic solar cell devices with photoactive layers of PBDTTT-CT: PDI (3:7) blend system annealed at 100 °C, with different vol. % of DIO additive. In all cases the device structure was glass/ITO/ZnO/PBDTTT-CT: PDI/V_2O_5/Ag. All data are reported after averaging the results obtained by at least three different devices.

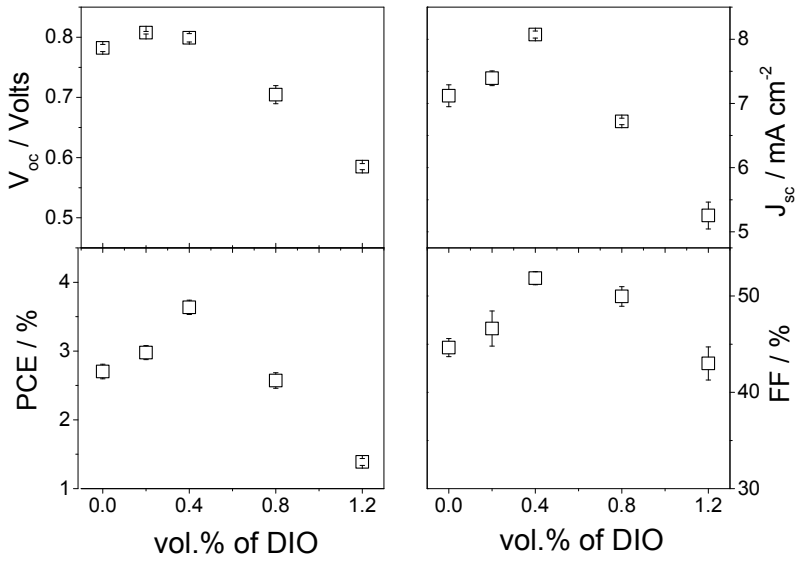

Figure S.3 The main figures of merit for organic solar cell devices with photoactive layers of PBDTTT-CT: PDI (3:7) blend system annealed at 100 °C, with different vol. % of DIO additive. In all cases the device structure was glass/ITO/ZnO/PBDTTT-CT: PDI/V_2O_5/Ag. All data are reported after averaging the results obtained by at least three different devices.

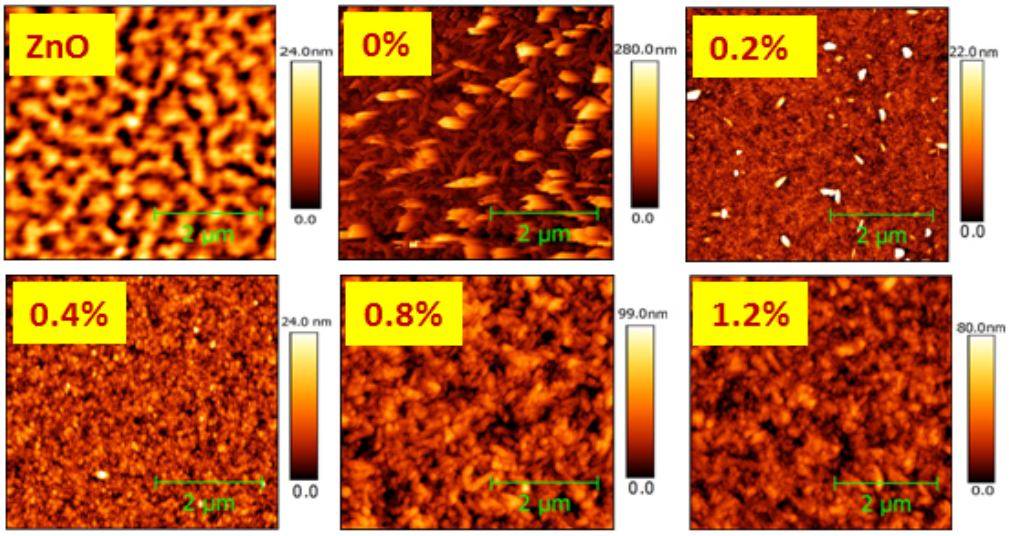

Figure S.4 Atomic force microscope images of PBDTTT-CT:PDI (3:7) blend films annealed at 100 °C with different vol. % of DIO additive, acquired with a scan length of 5 µm. In all the cases films were spin coated on the top of glass/ITO/ZnO in an identical fashion as the corresponding solar cell devices were fabricated.

Table S.1 Roughness of the films measured for 5 x 5 μm² scan area :

Sample	Rms (nm)	Avg (nm)	PDI aggregate Size (length × width in μm²)
ZnO	3.31	4.01	-
0%	28	42	0.045
0.2%	1.65	3.67	0.017
0.4%	1.95	2.53	0.013
0.8%	5.72	7.24	0.031
1.2%	8.01	10.18	0.032

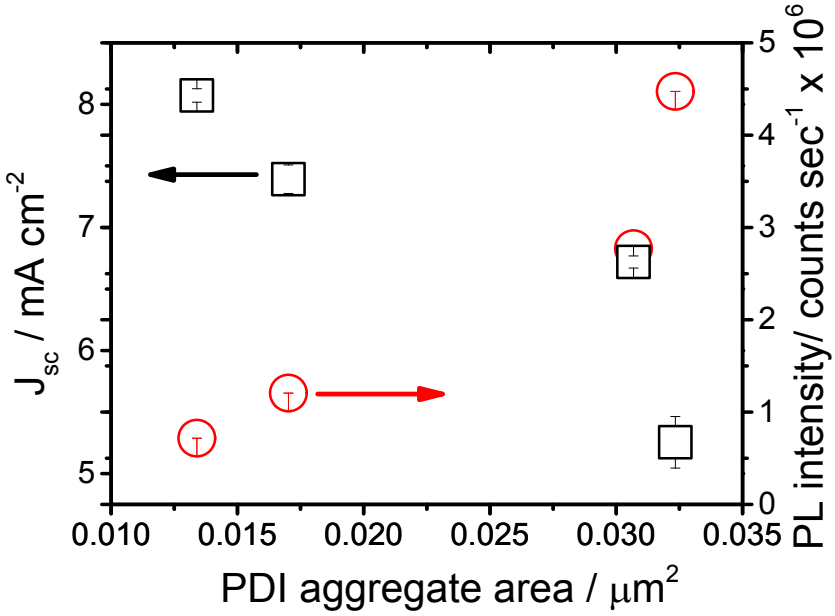

Figure S.5 The spectrally integrated PL intensity (λ_{range} = 560-720nm) (circles) of PBDTTT-CT:PDI w/DIO films as the areal size of the PDI aggregates in PBDTTT-CT: PDI (3:7) blend system varies by changing the vol. % of the DIO content in the film. The dependence of the short-circuit photocurrent density of the corresponding devices on the PDI aggregate areal size also shown (squares).

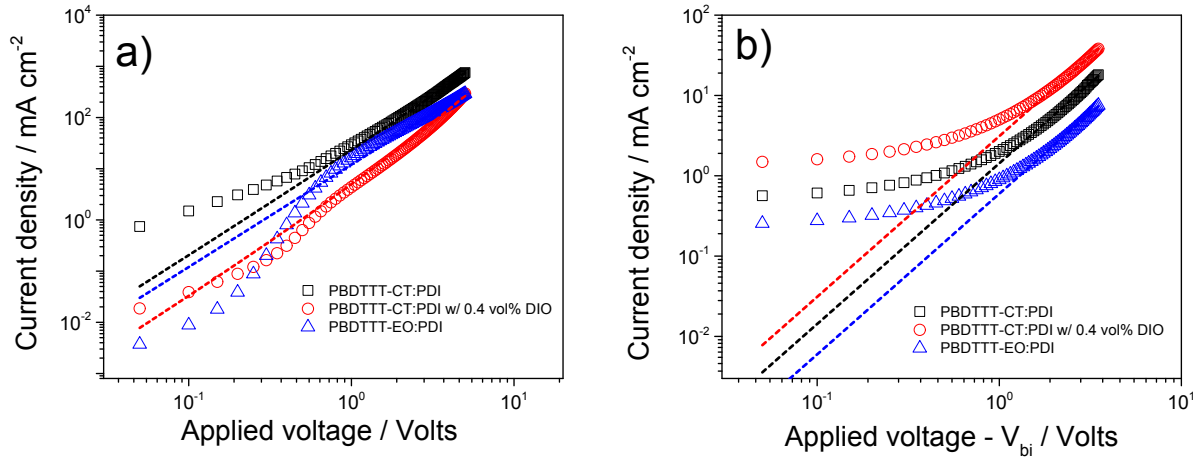

Figure S.6 Dark *J-V* curves of a) hole-only glass/ITO/PEDOT:PSS/PBDTTT-CT:PDI (3:7)/Au and ITO/PEDOT:PSS/PBDTTT-EO:PDI (3:7)/Au devices and b) electron-only glass/ITO/ZnO/PBDTTT-CT:PDI (3:7)/Ca/Al and ITO/PEDOT:PSS/PBDTTT-EO:PDI (3:7)/Au devices, with photoactive layers annealed at 100 °C without and with DIO vol% content of 0.4. For the case of the electron-only devices the build-in voltage value of V_{bi} =1.5 Volts was used. The dashed lines are fits to the experimental data according to Eq. S.1

$$J(V) = \frac{9}{8}\varepsilon_0\varepsilon_r\mu_0 \exp(0.89\gamma\sqrt{V/L})\frac{V^2}{L^3}, \quad \text{(Eq. S.1)}$$

Zero-field mobility, $\mu \propto$ cm^2/(V sec)
Film thickness, L $\propto$ cm
Dark current density J $\propto$ mA/cm^2
Voltage, V $\propto$ Volts
Vacuum permittivity, $\varepsilon_0 = 88.54 \times 10^{-12}$ (mA sec)/(V sec)
Dielectric constant, ε_r=3

Table S.2 Hole mobility of the hole-only glass/ITO/PEDOT:PSS/PBDTTT-CT:PDI (3:7)/Au and devices with photoactive layers annealed at 100 °C, without and with DIO vol% content of 0.4. The hole-mobility for the glass/ITO/PEDOT:PSS/PBDTTT-EO:PDI (3:7)/Au device is also reported.

System	$<\mu_h>$ (cm^2/Vsec)	$\pm sd_h$ (cm^2/Vsec)
PBDTTT-CT:PDI	8.26×10^{-5}	1.37×10^{-5}
PBDTTT-CT:PDI w/ 0.4% DIO	5.44×10^{-6}	1.94×10^{-6}
PBDTTT-EO:PDI	4.70×10^{-5}	4.41×10^{-6}

Table S.3 Electron mobility of the electron-only glass/ITO/ZnO/PBDTTT-CT:PDI (3:7)/Ca/Al devices with photoactive layers annealed at 100 °C, without and with DIO vol% content of 0.4. The electron-mobility for the glass/ITO/ZnO/PBDTTT-CT:PDI (3:7)/Ca/Al device is also reported.

System	$<\mu_e>$ (cm^2/Vsec)	$\pm sd_e$ (cm^2/Vsec)
PBDTTT-CT:PDI	6.41×10^{-6}	7.76×10^{-7}
PBDTTT-CT:PDI w/ 0.4% DIO	7.56×10^{-6}	1.52×10^{-6}
PBDTTT-EO:PDI	2.90×10^{-6}	1.04×10^{-7}

References

1 T. Ye, R. Singh, H.-J. Butt, G. Floudas, P. E. Keivanidis, ACS Appl. Mater. Interfaces 2013, **5**, 11844

2 Y. Sun, J.-H. Seo, C. J. Takacs, J. Seifter, A. J. Heeger, Adv. Mater. 2011, **23**, 1679

3 I. Hancox, L. A. Rochford, D. Clare, P. Sullivan, T. S. Jones, Appl. Phys. Lett. 2011, **99**, 013304